RAA 2019 Vol. **19** No. **1**, 2(8pp) doi: 10.1088/1674–4527/19/1/2

http://www.raa-journal.org *http://iopscience.iop.org/raa*

***R**esearch in*
***A**stronomy and*
***A**strophysics*

Repercussions of solar high energy protons on ozone layer during super storms

Asheesh Bhargawa, Mohd Yakub and Ashok Kumar Singh

Department of Physics, University of Lucknow, Lucknow-226 007, India; *asheeshbhargawa@gmail.com*

Received 2017 December 22; accepted 2018 June 8

Abstract We are very aware of the importance of the ozone layer, without which life on the Earth would not have evolved in the way it has. Solar storms carry energetic protons into the Earth's upper atmosphere, where they boost production of nitrogen oxides which are known as ozone killers and which ultimately increase ultraviolet (UV) radiations. In the present study, we estimate the effects of solar energetic protons during super storms (Dst index < -300 nT) over the total ozone column for the last 32 yr. We select a total of seven super storm events that occurred during solar cycles 22–24 (for the last 32 yr) having Dst index < -300 nT. To that end, we apply superposed epoch analysis (SEA) to verify the impact of storm events on the quantitative variation of total ozone column and on UV radiations during super storm events. After completing the empirical analysis, we conclude that the ozone column gets depleted significantly ($22\pm6.8\%$) as proton density increases during super storm events and this decrement in the ozone level is further responsible for a substantial increase ($26\pm11.2\%$) in peak UV radiation intensities.

Key words: Sun: particle emission — Sun: solar terrestrial relations — Sun: astroparticle physics — Sun: Physical Data and Processes

1 INTRODUCTION

The radiation environment of the Earth's atmosphere is very dynamic and consists of several components of ionizing radiation. Streams of particles from the Sun in combination with extreme space weather conditions have an influential impact on the Earth and its climate (Singh et al. 2010; Siingh et al. 2011; Singh & Tonk 2014; Singh et al. 2014). One of the most severe factors responsible for radiations is solar energetic particles (SEPs). SEPs are high energy (keV–GeV) particles consisting of protons, electrons and HZE ions. (HZE ions are the high-energy nuclei component of Galactic cosmic rays which have an electric charge greater than +2. The abbreviation "HZE" comes from high (H) atomic number (Z) and energy (E)). Significant SEP sources in the interplanetary medium are solar flares and shock waves driven by coronal mass ejections (CMEs) (Reames et al. 1996; Reames 1999; Gosling et al. 2005). The generation processes, flux density structures, spatial and temporal variations and energy distributions of each of these particle populations significantly differ from each other (Svestka & Simon 1976; Tascione 1988; Vainio et al. 2009). Sometimes, the density structures of the extended corona and preexisting energetic particles also influence the production of SEPs (Gopalswamy et al. 2004; Kahler & Vourlidas 2005).

The disturbance storm time index (Dst index,) expressed in nanotesla (nT), is a measure of geomagnetic activity to assess the severity of storms. It is based on the average value of the horizontal component of Earth's magnetic field measured hourly at four near equatorial geomagnetic observatories. It gives information about the strength of the ring current around the Earth caused by solar protons and electrons (Dungey 1961; Sugiura 1963; Tsurutani et al. 1992; Gonzalez et al. 1994). The enhanced solar wind magnetosphere energy coupling is responsible for the production of geomagnetic storms (Sugiura 1963). These storms may be classified in various categories (Tsurutani et al. 1992) but in the present case we have considered only super storms (Dst < -300 nT).

Scientists have been puzzled by the chemical processes that destroy ozone molecules in the stratosphere. Even the reactions with chlorofluorocarbons (CFCs) which are responsible for ozone depletion in the lower stratosphere could not explain the decline in ozone at higher layers. The ozone layer, an important part of Earth's atmosphere which contains relatively high concentrations of

ozone (O_3), absorbs 93%–99% of ultraviolet (UV) radiation coming from the Sun and prevents damage to life on Earth (Albritton 1998).

Normal ozone concentration is about 300 to 350 Dobson unit (DU). Apart from other reasons (the presence of higher concentrations of CFCs in the atmosphere), SEPs during solar storms are also responsible for the decline of ozone concentration (Hadjinicolaou et al. 2005). Sometimes, an increased density of protons in the upper atmosphere breaks the molecules of gases like nitrogen and water vapor that react with ozone molecules and reduce the ozone column (Damiani et al. 2009). When nitrogen gas molecules split apart due to SEPs, they can create molecules of nitrogen oxides that can last several weeks to months depending on where they end up in the atmosphere and sometimes when atmospheric winds blow them down into the middle atmosphere, they can stay there for months and continue to keep ozone at a reduced level (Manney et al. 2011). Recently, Verronen & Lehmann (2013) studied the effect of extreme particle precipitation and also outlined some of the chemical changes that occur during SEPs. They have also drawn links between geomagnetic activity and particle precipitations.

In the present paper, we analyze how the SEPs create an imbalance in the process of natural production and loss of the ozone column content and ultimate enhancement in UV radiations during storm days. In order to determine the variations in ozone levels and UV increment during the solar storms (proton events), we have chosen a total of seven of the most powerful super solar storms (Dst< -300 nT) that occurred during solar cycles 22, 23 and 24 (for the last 32 yr). We look for the impact of solar proton density and ultimately a significant depletion in the ozone column. We use the superposed epoch analysis (SEA) method to establish the credibility of the result for each event. The SEA method was first introduced by Chree (1913a,b). For investigating the possible relationship between two sets of geophysical observations, he introduced a procedure for analyzing one set of measurements during epochs that were selected based on a specific type of feature in the second set of measurements. Further, the SEA method has been utilized by several groups for investigating solar rotation and solar oscillations (Grec et al. 1980), periodic and non-periodic perturbations in the geo-magnetosphere (Iyemori & Rao 1996; Kamide et al. 1998), solar wind, interplanetary magnetic field and cosmic ray variations in the heliosphere (Meyer & Simpson 1954; Badruddin 2002), variation of temperature profile and wind characteristics in the atmosphere (Pudovkin et al. 1997), changes in ozone contents in the stratosphere and cloud behavior in the troposphere (Kniveton & Todd 2001).

We have also studied the variations in UV radiations during SEPs and storm events. Actually, the level of UV radiations on the Earth's surface is generally described by the UV index, which is derived from the convolution of surface UV irradiance with the thermal action spectrum (McKinlay & Diffey 1987) and ranges from zero (when no Sun is present) to more than 15 at midday in certain tropical regions (Guilbert 2003). As the ozone layer is depleted, there are also long term variations in the UV index. We have also applied the SEA method to UV index data obtained during the above considered storm days and found an increment in the UV index level.

To implement the SEA method, we selected a total of seven already mentioned super storm events that occurred during the last 32 yr. The present paper is divided into various sections. Section 1 of the manuscript deals with the introductory part while Section 2 describes the observational data sources, and their interpretation and analysis. Results and discussions are presented in Section 3 and final conclusions are presented in Section 4.

2 DATA SOURCES, INTERPRETATION AND ANALYSIS

The hourly values of Dst index were obtained from the World Data Center for Geomagnetism at the University of Kyoto (*http://wdc.kugi.kyoto-u.ac.jp/dst_final/index.html*), while hourly data of solar wind proton density used in this study were obtained from the GOES-11 satellite available on NASA's Space Physics Data Facility (*https://spdf.gsfc.nasa.gov/data_orbits.html*). For ozone, the database used consists of hourly values of the total ozone column amount in DU for the years 1986 to 2016, which were obtained from the Total Ozone Mapping Spectrometer (TOMS) at the Toronto station in Canada (Lat. 43°45′, Long. 79°24′ and available on World Ozone and Ultraviolet Radiation Data Centre (WOUDC, *http://woudc.org/data/explore.php*)). Data on the UV index were also taken from the same Toronto station, which is available on the WOUDC website.

UV radiation spans the wavelength range of 100–400 nm and is divided into three bands, namely UV-A (315–400 nm), UV-B (280–315 nm) and UV-C (100–280 nm). As sunlight passes through the atmosphere, all UV-C and approximately 90% of UV-B radiation are absorbed by ozone, water vapor, oxygen and carbon dioxide (Park et al. 2017). UV-A radiation is less affected by the atmosphere. Therefore, the UV radiation reaching the Earth's surface is largely composed of UV-A with a small

UV-B component. Depletion of the ozone layer is likely to aggravate existing health effects caused by exposure to UV radiation. As the ozone layer becomes thinner, the protective filter provided by the atmosphere is progressively reduced. Consequently, human beings and the environment are being exposed to higher UV radiation levels, and especially higher UV-B levels that have the greatest impact on human health, animals, marine organisms and plant life (Damiani et al. 2014). A UV index reading of 0 to 2 means low danger, 3 to 5 means moderate risk and 6 to 7 means high risk of harm from unprotected Sun exposure. A UV index reading of 8 to 10 means very high risk of harm from unprotected Sun exposure (Mead 2008).

As mentioned earlier, we have considered seven super storm events with intensity less than -300 nT and have analyzed the variation of solar proton and total ozone column characteristics.

Table 1 lists the date and time (UT) of each super storm event. Further, the effect of solar storms on the total ozone column has been estimated using SEA. The basic idea of SEA is to test for a significant relationship between the occurrence of a super storm event (key event) and variation in total ozone column during corresponding days (key response). The superposed epoch is a row-column array in which the 'response' index values filling any row form the data pertaining to a single key event. Thus, the number of rows is the sample size for such events. The columns compose the index values in fixed time relation to the key times and the column average comprises the "superposed epoch analysis." By this averaging method, any fluctuations in the response index that correspond in time relative to the key time column are preserved in the average, whereas fluctuations shifting in time from row to row are averaged out. Before constructing a superposed epoch and analyzing it, consideration should be given to the two types of data that enter such analysis: the sample of key times and the response index that is superposed on these times.

In fact, the SEA method (Chree 1913a,b) is a statistical method used to resolve significant signal to noise problems. This is especially desired in cases where the responses to particular events may be unclear by noise from other competing influences that operate at similar time scales. Through simple compositing, the SEA method involves sorting data into categories dependent on a 'key-date' for synchronization and then comparing the means of those categories. Given sufficient data, a common underlying (causal) response to a forcing event should theoretically emerge in the average (composite) while other noise in the data should cancel. Examples of applications of the SEA method are widespread in various scientific fields of study (Brier & Bradley 1964; Mass & Portman 1989; Swetnam & Betancourt 1990; Lühr et al. 1998).

Table 1 List of occurrence times and peak values of Dst index, solar proton density, total ozone column and UV index for all seven events under consideration.

S. No.	Dst Index		
	Date	Time (UT)	Min. Value (nT)
1	09–02–1986	01:00	–307
2	14–03–1989	02:00	–589
3	09–11–1991	02:00	–354
4	16–07–2000	01:00	–301
5	31–03–2001	09:00	–387
6	20–11–2003	22:00	–422
7	08–11–2004	07:00	–374
	Solar Proton Density		
	Date	Time (UT)	Max. Value (cm^{-3})
1	09–02–1986	16:00	97.80
2	14–03–1989	18:00	55.64
3	09–11–1991	13:00	32.00
4	16–07–2000	11:00	32.80
5	31–03–2001	23:00	38.20
6	20–11–2003	23:00	22.10
7	08–11–2004	19:00	89.20
	Total Ozone Column		
	Date	Time (UT)	Min. Value (DU)
1	09–02–1986	14:00	298.8
2	14–03–1989	23:00	324.2
3	09–11–1991	23:00	253.1
4	16–07–1991	06:00	299.5
5	31–03–2001	18:00	289.3
6	20–11–2003	23:00	212.7
7	08–11–2004	19:00	221.0
	UV Index		
	Date	Time (UT)	Peak Value
1	09–02–1986	12:30	6.43
2	14–03–1989	11:18	6.39
3	09–11–1991	12:57	6.14
4	16–07–2000	13:40	5.36
5	31–03–2001	11:10	5.72
6	20–11–2003	11:49	5.24
7	08–11–2004	13:24	5.81

3 RESULTS AND DISCUSSION

SEPs may be associated with flares and CMEs that occur when protons with very high energy are emitted by the Sun during solar storm events. High energy solar protons penetrate the Earth's magnetic field and typically reach 80 to 40 km into the atmosphere (Akasofu 2011). In this way, they provide a direct connection between the Sun and the Earth's middle atmosphere (Seppälä et al. 2004). In this

context, geomagnetic storms are probably the most important phenomenon related to solar wind and high energy particles (Singh et al. 2010). They produce large disturbances in the ionosphere and also affect the neutral atmosphere including the lower atmosphere, so we can expect them to affect the total ozone as well as the ozone profile.

In the present study, we have chosen seven super storm events that occurred during solar cycles 22 (1986–1996), 23 (1996–2008) and 24 (2008–present), with Dst<-300 nT, and have analyzed the impact of SEP events on the ozone column and on the UV radiation level.

Table 1 presents the details of all these seven events and lists the occurrence time and peak values of Dst index, solar proton density, total ozone column and the value of UV index during the storm event, from top to bottom respectively.

3.1 Super Storm Events (Dst < -300)

We have plotted all seven storm events together in Figure 1. The first case of a super storm was recorded on 1986 February 9 and was associated with a number of solar flares with low intensities that occurred. The peak of the storm was observed at 01:00 UT on February 9. By chance, this storm was the largest recorded storm since 1960 and the eighth largest since 1932 (Allen 1986). Two other factors made this storm particularly unusual: (i) it happened near the minimum in the Sun's activity cycle; and (ii) it was apparently caused by flares that could be described as moderate to large. The initial phase of this storm started on Feb 6 at 21:00 UT and continued till Feb 07 at 07:00 UT, and the main phase occurred with its minimum value (Dst index -307 nT) on Feb 9 at 01:00 UT, then it reached its recovery phase and this phase continued till Feb 13 at 23:00 UT. The second event of the considered solar storm was observed on 1989 March 14. This storm was the result of a large CME. During this storm, prolonged proton events transpired, which lasted for several days and had an unusually high proportion of energetic particles.

Figure 1 (Case 2) presents a detailed depiction of the variation in Dst index for the period 1989 March 11–17. The variation in Dst index during the super storm reached its minimum value of -589 on March 14 at 02:00 UT. The third event associated with the super storm occurred on 1991 November 9. During this large storm, the minimum hourly Dst reached -354 nT at 02:00 UT.

Figure 1 (Case 3) displays the variation of Dst index for the period 1991 November 6–12. Figure 1 (Case 4) illustrates the variation in Dst index for the fourth event that happened from 2000 July 13–19. We observe a very intense fall in the Dst index, reaching a minimum of -301 nT at 01:00 UT on July 16 and this minimum sustained for almost one hour. The fifth case of a super storm was recorded on 2001 March 31 and was a result of a fast solar wind transient with a strong southward interplanetary magnetic field B_z.

Figure 1 (Case 5) presents the variation of Dst index for the period of 2001 March 28 to April 3. The figure clearly indicates that Dst reached its minimum of -387 nT during 03:00–09:00 UT and this storm was the result of an intense solar flare associated with a large CME. In Case 6, we demonstrate the variation of Dst index for the period from 2003 November 17–23. This case of a super storm event was recorded on 2003 November 20 with a minimum Dst value of -422 nT during 21:00–22:00 UT. The seventh super storm event was recorded on 2004 November 8 and Dst reached its minimum value of -374 nT at 07:00 UT, with a partial recovery and a further increase in the absolute value of Dst index of -259 nT on November 10 at 08:00 UT.

3.2 Solar Proton Density Variations during Super Storms

Figure 2 shows the variations in solar proton density during the seven storm events, which are denoted as Case 1 to Case 7 respectively. The variations in solar wind proton density during the first event have been displayed as Case 1 in Figure 2. A sudden increase in the proton density is observed just after the peak of the storm and reaches its maximum value of 97.8 cm^{-3} on Feb 9 at 16:00 UT and finally decreases to the value 10.2 cm^{-3} by 21:00 UT. During the second storm event, the value of solar wind proton density starts increasing suddenly after the storm and attains its maximum value of 55.64 cm^{-3}. The third storm was responsible for the sudden increase in solar wind proton density that was recorded at 13:00 UT with a maximum value of 32.0 cm^{-3}. But in the case of the fourth storm, we observed contradictory results as compared to the earlier ones. Here we identify enhancement in proton density before the storm event. In fact, we notice four peaks associated with Case 4 in the figure. The first peak occurred at 11:00 UT on July 13 with its maximum value of 32.80 cm^{-3} while the second one was recorded at 23:00 UT on July 14, the third one occurred at 18:00 UT on July 15 and the last one happened on July 16 at 11:00 UT. This contradiction might be because this storm occurred during a peak period of the 23$^{\rm rd}$ solar activity cycle and was driven by a powerful CME associated with an X 5.7 class flare. Due to these high solar activity conditions, solar radiation storms occurred and were responsible for multiple peaks (Singh & Tonk 2014). As a consequence of the

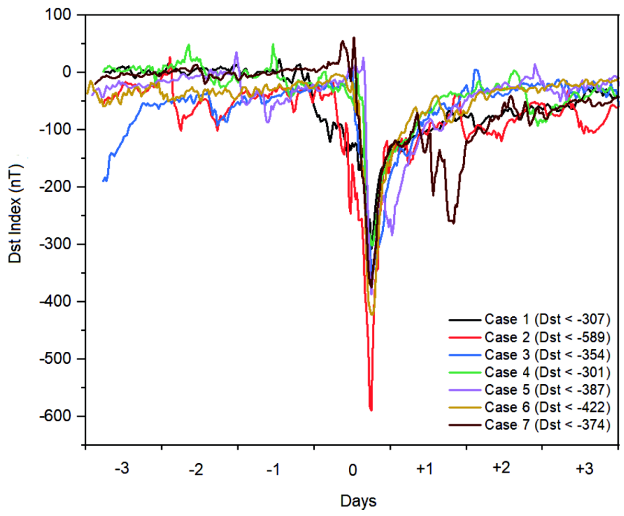

Fig. 1 Variation of Dst index for all seven events selected for the study. The super storm day is assigned as 0 (zero), and + and – indicate the subsequent post- and pre- storm days respectively.

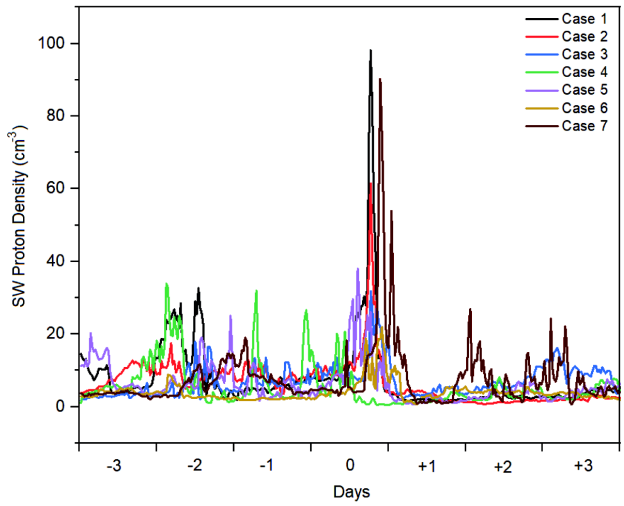

Fig. 2 Solar proton density variation during the same storm events investigated in this study. The super storm day is assigned 0 (zero), and + and − indicate the subsequent post- and pre-storm days respectively.

fifth storm, the flux of protons toward Earth's atmosphere was greatly enhanced as evident in the figure (Case 5). A solar proton event reached its peak value of 38.2 cm^{-3} at 23:00 UT on March 31. On the same day that the sixth storm event happened, a significant increase in solar wind proton density was observed at a level of 22.10 cm^{-3} at 23:00 UT and Case 7 exhibits temporal evolution of the Dst index during the period 2004 November 5–11. The solar protons reached their maximum value of 89.2 cm^{-3} at 19:00 UT on November 8.

3.3 Total Ozone Column Change during Super Storms

In Figure 3, the variation of ozone column during all seven storm events is plotted all together. During the occurrence of the first storm event, the total ozone column also showed some consistent variation with this sudden change in proton density. A sudden decrease in total ozone column was observed and the content reached to its minimum of 298.8 DU (roughly 25% depletion) on Feb 9 at 14:00 UT, and this decrease continued till Feb 11 at 03 UT. As a result of enhancement in proton density during the second storm, we also observed a sudden decrement in total ozone column which reached its minimum value of 324.2 DU and we noticed about a 19% depletion in ozone column as shown in Figure 3. This sudden decrease in the ozone content during the solar storm event sustained till March 14 at 23:00 UT. With the result of this increase in proton density during the third storm event, the total ozone column started decreasing and reached its minimum value of 253 DU at 23:00 UT on November 9. Here we noticed about a 20% depletion in ozone content. After its minimum, the ozone level started to recover to its normal value. As far as depletion in the ozone column during the fourth storm event was concerned, it also started before storm commencement and reached its minimum value of 298 DU at 6:00 UT on the storm day, and we noticed about a 10% depletion in ozone column. As a result of the increase in proton density during the fifth storm event, the total ozone column started decreasing and reached its minimum value of 289 DU at 18:00 UT on 31 March. We noticed about a 27% depletion in ozone column as shown in the upper panel of the figure. The total ozone column during the sixth storm event showed a significant decrement and reached its minimum value of 212.7 DU at 23:00 on November 20 with 29% depletion in ozone column. As a result of the seventh storm event, a sudden decrease in the total ozone column was observed with its minimum value of 221 DU at 19:00 UT on November 8. Here we noticed about a 21% depletion in ozone column.

3.4 Variations in UV Index during Super Storms

The strongest solar flares are almost always correlated with CMEs and most of the intense storms result from conditions associated with CMEs. We have plotted the variation curves of the daily maximum UV index for the same time period as selected for the storm events.

Figure 4 illustrates all seven curves of UV index. From the figure, we observed that UV enhancements started a few days before the SEPs hit and the peak enhancement is

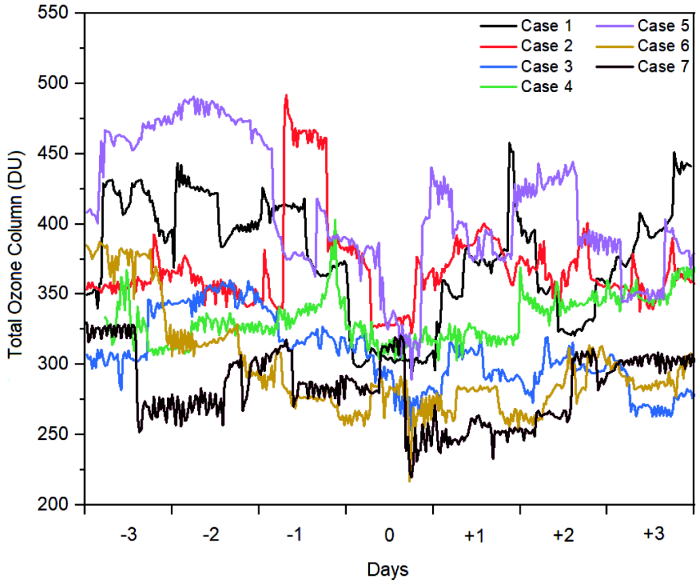

Fig. 3 Total ozone column variation during chosen storm events. The super storm day is assigned as 0 (zero), and + and – indicate the subsequent post- and pre- storm days respectively.

on the day of the SEP event. These prior enhancements in UV index may be a confluent effect of both the UV radiation from the solar flare (UV radiation from the Sun briefly went up by factors of thousands during solar flares) and solar protons (these solar protons were the indication of an eruptive solar event that likely launched a CME into space) ejected by it (Papaioannou et al. 2016). Thus enhancement in UV radiation at the surface of the Sun took part in the gradual increase of the UV index at the Earth, just after commencement of the solar flare. During huge explosions on the Sun (like a solar flare), a solar radiation storm can be triggered. Solar protons spread out into space and can travel nearly the speed of light in extreme events (Green et al. 2018). These protons are the first particles to arrive at Earth and can produce a minor destruction in atmospheric ozone layer that results in the gradual enhancement in the value of UV index. Therefore as a consequence of the above mechanisms, the UV index on the surface of the Earth started increasing on the day when a solar flare was observed, and on the day that the CME arrived at Earth (commencement of SEP), the UV index reached its peak.

During the storm day, the value of UV index reaches its peak value and after that it starts decreasing. The peak values of all curves are listed in Table 1. We compare these peak values with values of the UV index from the previous days which were non-storm days. During the first storm event, we observed an increment of 28% in the the UV index level; the second storm caused an increment of 21% in the UV index level. An increment of 32% was observed during the third storm and the fourth storm caused an increment of 24% in UV level. The effects of the fifth and sixth storm events also caused increments of 18% and 39% respectively. In addition, the seventh storm event increased the UV index level by 26%.

As discussed above, in all seven cases that have been considered, we observed that the decrement in total ozone column resulted from the corresponding sudden increment in proton density, so super storm activity was the main factor responsible for the sudden destruction of ozone content. The decrement in ozone column might be associated with the fact that when protons from the Sun hit the atmosphere, they break apart both water vapor and nitrogen gas. The nitrogen gas molecules (N_2) disconnect and leave two free nitrogen atoms. These atoms are highly reactive with O_2 and O, creating oxides of nitrogen. Once formed, these molecules can last for a few weeks to months depending on where they end up in the atmosphere. Protons also break up water vapor (H_2O) into a hydroxide molecule (OH) and a free-floating single atom of hydrogen. Both of these products also react easily with ozone and reduce its levels in the atmosphere (Jackman et al. 2008). Furthermore, during solar storm events, proton precipitation into the atmosphere caused the ozone depletion with an increase of NO_2 (Seppälä et al. 2004; Seppälä et al. 2006; López-Puertas et al. 2005). These constituents of NO_x ($NO+NO_2$) produced by solar proton events lead to a catalytic destruction of ozone.

We are well aware of the fact that a variation in the ozone column can result in a variation of the UV radiation level. Some past studies have already shown an inverse re-

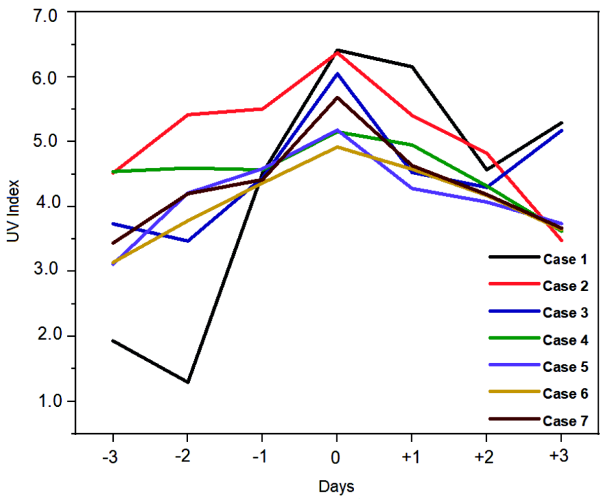

Fig. 4 Variation in daily maximum UV index during chosen storm events. The super storm day is assigned as 0 (zero), and + and − indicate the subsequent post- and pre- storm days respectively.

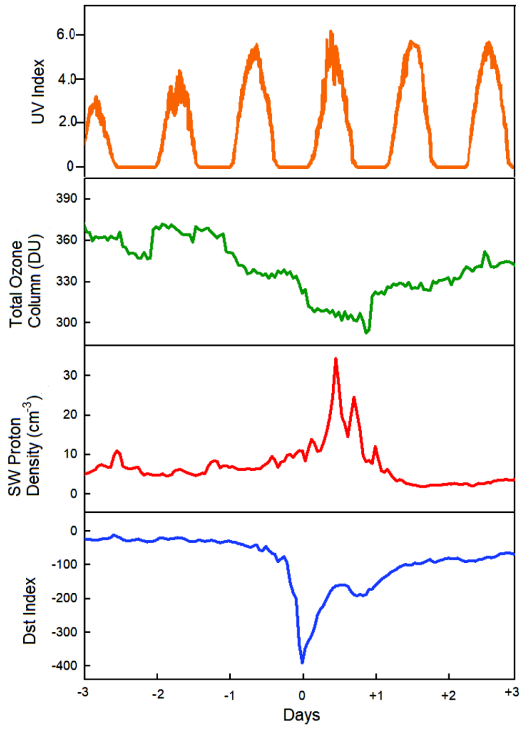

Fig. 5 The results of SEA have been described taking the super storm event as 0 (zero) day, and + and − indicate the subsequent post- and pre- storm days respectively.

lationship between ozone level and UV index (Albritton 1998; Herman 2010). They suggested that the depletion in ozone level due to anthropogenic factors results in the increase of UV index. A change in the ozone level during an intense storm is also important because it also increases the amount of UV radiation.

We have applied SEA (with details already given in Section 2) to these seven selected events to check the impact of a solar storm on ozone column depletion and also to confirm the variation level of the UV index during the storm event. The super storms forcing and total ozone column response data were incorporated into the SEA, which was used to evaluate the composite response of the total ozone column to super storm forcing events.

Figure 5 presents the overall result of SEA where it is clearly revealed that due to increased solar proton density during the storm period, we observed a roughly 22±6.8% decrement in the total ozone column and an increment of 26±11.2% was observed in the UV index. This confirmed the result obtained in all storm events considered except one where we observed the enhancement in proton density before commencement of a solar storm. The lower panel of the figure displays the variation in Dst index for seven days where '0' corresponds to the storm day while + and – mean the subsequent post- and pre-storm days respectively. Similarly, the second and third panels of the figure depict the resultant variation of solar proton density and total ozone column respectively. The upper panel presents the variation in UV index. From Figure 5 we have also observed that after the solar storm event solar proton density starts increasing, and after 10–12 hours it attained its peak. Similarly, a clear effect of the solar proton event on the total ozone column has been observed and there was a significant decrement in the total ozone content after proton density reached its maximum. Further, we noticed that depletion in the ozone column continued for 24–36 hours after the peak of the Dst index. This time delay in the observation of storm effects on the total ozone column might be associated with the delay in arrival of odd nitrogen or hydrogen molecules produced at higher altitudes (Rozanov et al. 2012). As a response to the reduction in ozone level, the UV index also showed an increment in its level (26±11.2%).

4 CONCLUSIONS

In the present paper, we have investigated the impact of solar storms on the total ozone column and ultimately on the variation of UV index. We have observed that the total atmospheric ozone was reduced up to 22± 6.8% after the storm events commenced. After analyzing the results of SEA, we found that when the super storms occurred, the density of solar energetic protons increased suddenly and this enhancement in proton density created an imbalance in the cycle of creation and destruction of the ozone content, and as a result a sudden decrement in the total ozone column was observed. As the ozone layer works as a shield

for UV radiation, a variation in its level leads to a fluctuation in the value of UV radiation coming towards Earth. Therefore, it is clear that during the storm days, the level of ozone column decreases due to bombardment of energetic particles, which results in a slight increase in the value of UV radiation during super storm days.

Acknowledgements Authors are thankful to various data providers like
http://wdc.kugi.kyoto-u.ac.jp/dst_final/index.html;
https://spdf.gsfc.nasa.gov/data_orbits.html
and *http://woudc.org/data/explore.php*.
AB is thankful to the University Grants Commission (UGC) for providing financial support in the form of the Rajiv Gandhi National Fellowship.

References

Akasofu, S.-I. 2011, Space science reviews, 164, 85
Albritton, D. 1998, in Protecting the Ozone Layer (Springer), 67
Allen, J. H. 1986, Eos, Transactions American Geophysical Union, 67, 537
Badruddin. 2002, solar physics, 209, 195
Brier, G. W., & Bradley, D. A. 1964, Journal of the Atmospheric Sciences, 21, 386
Chree, C. 1913a, Some Phenomena of Sunspots and of Terrestrial Magnetism at Kew Observatory, Philos, Tech. rep., Philosophical Transactions Royal Society London Series
Chree, C. 1913b, Some Phenomena of Sunspots and of Terrestrial Magnetism II, Tech. rep., Philosophical Transactions Royal Society London Series
Damiani, A., Cordero, R. R., Cabrera, S., Laurenza, M., & Rafanelli, C. 2014, Atmospheric Research, 138, 139
Damiani, A., Diego, P., Laurenza, M., Storini, M., & Rafanelli, C. 2009, Advances in Space Research, 43, 28
Dungey, J. W. 1961, Physical Review Letters, 6, 47
Gonzalez, W. D., Joselyn, J. A., Kamide, Y., et al. 1994, J. Geophys. Res., 99, 5771
Gopalswamy, N., Yashiro, S., Krucker, S., Stenborg, G., & Howard, R. A. 2004, Journal of Geophysical Research: Space Physics, 109, A12
Gosling, J., Skoug, R., McComas, D., & Smith, C. 2005, Journal of Geophysical Research: Space Physics, 110, A1
Grec, G., Fossat, E., & Pomerantz, M. 1980, Nature, 288, 541
Green, L. M., Török, T., Vršnak, B., Manchester, W., & Veronig, A. 2018, Space Sci. Rev., 214, #46
Guilbert, J. 2003, Education for Health (Abingdon, England), 16, 230
Hadjinicolaou, P., Pyle, J. A., & Harris, N. R. P. 2005, Geophys. Res. Lett., 32, L12821
Herman, J. R. 2010, Journal of Geophysical Research: Atmospheres, 115
Iyemori, T., & Rao, D. 1996, Annales Geophysicae, 14, 608
Jackman, C., Marsh, D., Vitt, F., et al. 2008, Atmospheric Chemistry and Physics, 8, 765
Kahler, S. W., & Vourlidas, A. 2005, Journal of Geophysical Research (Space Physics), 110, A12S01
Kamide, Y., Yokoyama, N., Gonzalez, W., et al. 1998, J. Geophys. Res., 103, 6917
Kniveton, D. R., & Todd, M. C. 2001, Geophysical Research Letters, 28, 1527
López-Puertas, M., Funke, B., Gil-López, S., et al. 2005, Journal of Geophysical Research (Space Physics), 110, A09S43
Lühr, H., Rother, M., Iyemori, T., Hansen, T., & Lepping, R. 1998, Annales Geophysicae, 16, 743
Manney, G. L., Santee, M. L., Rex, M., et al. 2011, Nature, 478, 469
Mass, C. F., & Portman, D. A. 1989, Journal of Climate, 2, 566
McKinlay, A. F., & Diffey, B. L. 1987, CIE journal, 6, 17
Mead, M. N. 2008, Environmental Health Perspectives, 116, A160
Meyer, P., & Simpson, J. A. 1954, Physical Review, 96, 1085
Papaioannou, A., Sandberg, I., Anastasiadis, A., et al. 2016, Journal of Space Weather and Space Climate, 6, A42
Park, S. S., Kim, M., Lee, H., et al. 2017, Atmosphere, 8, 109
Pudovkin, M., Veretenenko, S., Pellinen, R., & Kyrö, E. 1997, Advances in Space Research, 20, 1169
Reames, D., Barbier, L., & Ng, C. 1996, The Astrophysical Journal, 466, 473
Reames, D. V. 1999, Space Science Reviews, 90, 413
Rozanov, E., Calisto, M., Egorova, T., Peter, T., & Schmutz, W. 2012, Surveys in geophysics, 33, 483
Seppälä, A., Verronen, P., Kyrölä, E., et al. 2004, Geophysical Research Letters, 31, 19
Seppälä, A., Verronen, P. T., Sofieva, V. F., et al. 2006, Geophys. Res. Lett., 33, L07804
Siingh, D., Singh, R., Singh, A. K., et al. 2011, Surveys in Geophysics, 32, 659
Singh, A. K., Siingh, D., & Singh, R. P. 2010, Surveys in geophysics, 31, 581
Singh, A., & Tonk, A. 2014, Astrophysics and Space Science, 353, 367
Singh, A., Tonk, A., & Singh, R. 2014, Indian Journal of Physics, 88, 1127
Sugiura, M. 1963, Ann. Int. Geophys., 35, 9
Svestka, Z., & Simon, P. 1976, Catalog of Solar Particle Events 1955–1969. Prepared under the Auspices of Working Group 2 of the Inter-Union Commission on Solar-Terrestrial Physics. 1975
Swetnam, T. W., & Betancourt, J. L. 1990, Science, 249, 1017
Tascione, T. F. 1988, Introduction to the Space Environment (Orbit Book Co. Inc. and Krieger Publishing Co., Melbourne)
Tsurutani, B. T., Gonzalez, W. D., Tang, F., & Lee, Y. T. 1992, Geophys. Res. Lett., 19, 73
Vainio, R., Desorgher, L., Heynderickx, D., et al. 2009, Space Science Reviews, 147, 187
Verronen, P. T., & Lehmann, R. 2013, Annales Geophysicae, 31, 909